AWARDS - 2000

Research Section: 1st Prize Winning Paper

Studies on characterization of high performance coatings based on polymer alloys of interpenetrating polymer networks

T. Anandaraj, P.S. Mohan, Sm. Krishnan, K. Balakrishnan & M. Raghavan

Corrosion Science and Engineering Division
Central Electrochemical Research Institute
Karaikudi 630 006, India

Abstract

Organic coatings are valued after the polymeric binder material out of which it is made for the reason that it only decides the extent of protection and the life of a coating.

Of a few ways to obtain better performing polymeric binders, alloying the incompatible polymers through 'compatibilization' is fast-emerging with a number of promises. Interpenetrating polymer networks are one of its kinds.

In this study, two polymer alloys of Interpenetrating Polymer Network (IPN) based on epoxy-acrylic-polyurethane polymers have been developed in the laboratory and subjected to different laboratory accelerated tests as pigmented coatings. They have been found to possess far superior physical and chemical and corrosion resistance properties compared to crosslinked acrylates, polyamide cured epoxies and polyurethanes.

The IPNs as clear coatings were also characterized by various physico-chemical and surface analytical techniques. The thermo-analytical techniques, FTIR and SEM confirmed the formation of IPN. The improved corrosion resistance properties were established by water permeation tests and electrochemical impedance spectroscopy.

Introduction

THE search for polymers providing better and better properties is ever lasting. In this aspect, Interpenetrating Polymer Networks, shortly IPNs, a class of polymer alloys promises a number of advantageous coating properties like corrosion resistance, chemical resistance and improved mechanical properties. IPNs are the resultant products of an attempt at compatibilization of two or more immiscible polymers to achieve a compatibilized polymer alloy [1-11]. These networks of various chemical natures constitute a new approach to the problem of mutual incompatibility of polymers, as both components are intimately combined in their network form during the synthesis itself. In this case, the morphology is somewhat 'fixed' (reported often as physical entanglement) as soon as all the chemical reactions have taken place [5-6].

The main advantages of these IPNs are that they are relatively not easily affected by external stresses (which happens to polymer blends made of simple physical mixing where the component polymers are not compatibilized). The IPNs also pos-

sess improved properties than two chemically dissimilar homo/neat polymers out of which they are made. An interesting property is that the end properties of the IPNs can be tailor made to suit any anticipated conditions [8-11].

In this study, two such IPNs have been, in semi-macro level, synthesized in the laboratory and their pigmented coatings were subjected various laboratory accelerated tests which convincingly brought out the better performing nature of the IPNs than the conventional systems such as crosslinked acrylics, polyamide cured epoxies and polyurethanes.

In this paper, the extensive characterization of the IPNs using different modern techniques such as scanning electron microscopy, FT-IR, gel permeation chromatography and thermal measurements has been extensively dealt with. The nature of IPNs assessed from their characterization has helped much in formulating them and making them as coatings for aggressive conditions.

Mr. T. Anandraj being felicitated by Prof. M.M. Sharma at the IPA Conference held on Feb. 9-11, 2001 in Chennai (IPA 1st Prize for his Research Paper)

Experimental studies

Synthesis of epoxy-acrylate precursors

In order to optimize the physico-chemical properties of the IPNs, epoxy-acrylate precursors with three different ratios, viz. 50:50, 65:35 and 35:65 of epoxy-urethane to acrylate were designed. The epoxy-acrylate precursors were synthesized using sequential polymerization processes. One set of epoxy-acrylate precursors, named as EA-F1, F2 and F3, were used to prepare Full-IPNs and another set of epoxy-acrylate precursors, named EA-G1, G2 and G3 were used to prepare the Grafted-IPNs. Likewise, the urethane crosslinker prepolymer was also synthesized in the laboratory using conventional methods with toluene diisocyanate and trimethylol propane/polyethylene glycols as the monomers.

Synthesis of IPNs

Two types of IPNs, viz. Full-IPNs (FIPN series) and Grafted-IPNs (GIPN series) with three different compositional ratios were synthesized. This was done by mixing a calculated quantity of the epoxy-acrylate precursor resins (epoxy-acrylate precursors EA-F1, -F2 and -F3 for full-IPNs of three different ratios and epoxy-acrylate precursors EA-G1, -G2 and -G3 for grafted-IPNs of three different ratios) with a known weight of urethane prepolymer crosslinker U-PP solution. The films were formed over a PTFE cloth / mild steel panels by a film applicator/spray and left to cure at ambient conditions for one week. The films were then tested for physical and chemical resistance properties.

Neat systems

To compare the performance behavior of the IPN systems with the neat polymer systems, three polymer systems, which were used to form the IPN structural backbones, were selected, viz. crosslinked acrylic copolymer system, polyamide cured epoxy system and acrylic polyol based aromatic polyurethane system.

Crosslinked acrylic copolymer system

A copolymer of butyl methacrylate/methyl methacrylate, butyl acrylate and 2-ethyl hexyl acrylate was prepared with ethylene glycol dimethacrylate as crosslinker. The cross-linked copolymer as 50% solution in xylene/toluene was used for NS-1C coatings.

Polyamide catalyzed epoxy system

To prepare the cold cured epoxy based neat system (NS-2C), commercial epoxy resin (Araldite GT6071-diglycidyl ether bisphenol-A based epoxy resin and epoxy equivalent 450-465) and polyamide crosslinker (Synpol-125 - polyamine reacted

TABLE 1: NOMENCLATURE OF COATINGS

Coating	Description
NS-1C	Neat system- Crosslinked acrylic copolymer
NS-2C	Neat system - Polyamide cured epoxy
NS-3C	Neat system - Acrylic polyol - aromatic polyurethane
FIPN-1C	Full IPN (Two component) Ratio 50:50
FIPN-2C	Full IPN (Two component) Ratio 65:35
FIPN-3C	Full IPN (Two component) Ratio 35:65
GIPN-1C	Grafted- IPN (Two component) Ratio 50:50
GIPN-2C	Grafted- IPN (Two component) Ratio 65:35
GIPN-3C	Grafted- IPN (Two component) Ratio 35:65

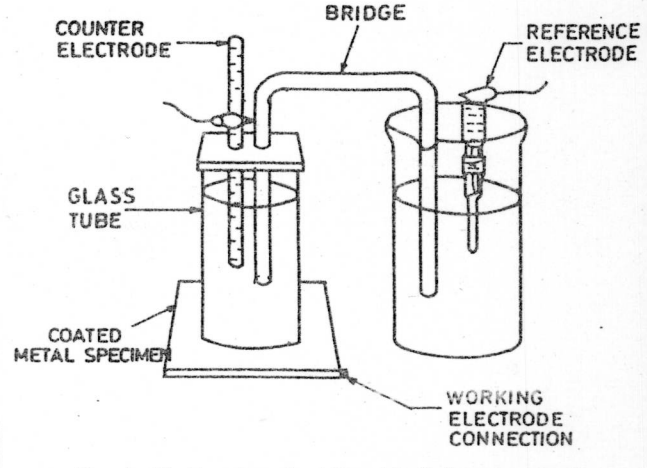

Fig. 1: Electrochemical Test Cell Arrangement

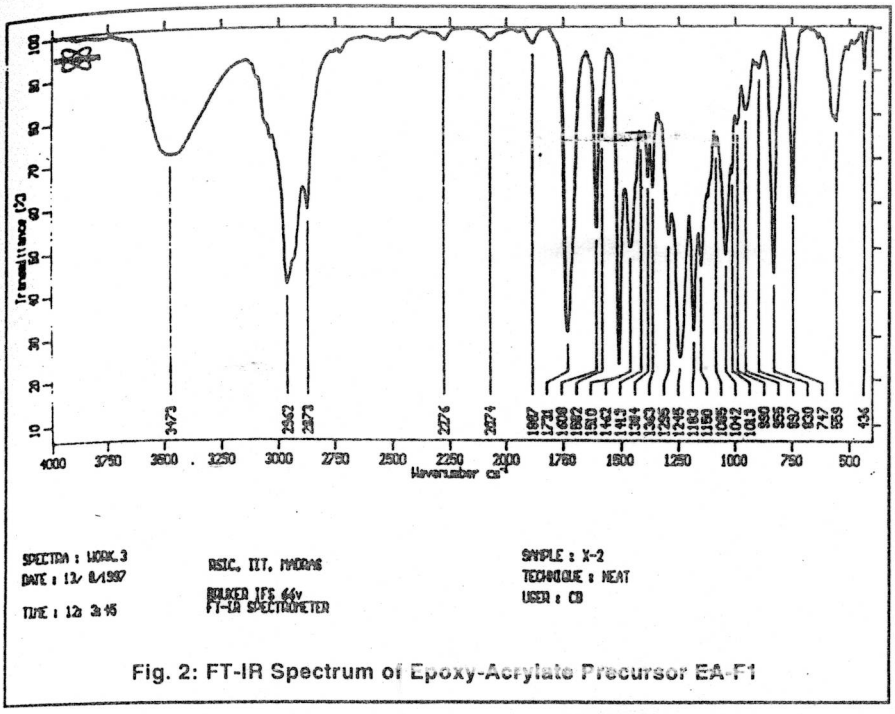

Fig. 2: FT-IR Spectrum of Epoxy-Acrylate Precursor EA-F1

dimerized tung Oil based crosslinker with amine value 280-320 mgm KOH) were used.

Acrylic polyol based aromatic polyurethane system

To prepare the acrylic polyol based aromatic polyurethane system (NS-3C), a commercial product of acrylic polyol (acrylic type with hydroxyl value 67-75) and aromatic isocyanate based urethane crosslinker (aromatic TDI based with NCO content 13% appr.) were used.

Nomenclature of coatings

Table-1 shows the various clear coatings used along with their description.

Specimen preparation

While for all studies on characterization, free films of the polymer alloys were used, for the AC-electrochemical impedance spectroscopic (EIS) studies, coatings applied over sand-blasted cold rolled cold annealed mild steel panels were used as working electrode.

Free-filming of IPNs

Free films of all the coatings have been prepared by applying the liquid coatings over a reinforced PTFE cloth using a film applicator and cured for seven days, after which the free film was slowly and carefully stripped/ peeled off and used for the studies of polymer characterization. No release agents like silicones were used for free-filming. The free films had a dry film thickness in the range of 40-50 microns with other optimum properties required for coatings.

Characterization methods

FT-IR Spectroscopy

For IR measurements, all the polymers in liquid form and in clear free film form were used by placing them in a cell formed by two sodium chloride windows separated by a PTFE gasket around 20 microns [12-14]. A *Bruker* IFS-66V software controlled FT-IR spectrometer was used wherein KBr pellet and neat techniques were employed.

Gel permeation chromatography

The number average molecular weight and polydispersity of all the polymer precursors and other resins [15] were determined using a software controlled GPC of *Shimatzu C-R4 A Chromatopac*, Japan make. The GPC made use of polystyrene as standard and the measurements were made at ambient conditions, with tetrahydrofuran as carrier solvent in a *Carbowax* column.

Scanning electron microscopy

For SEM studies, a software controlled scanning electron microscope, *Stereoscan 400 Version-2.02* supplied by *Leica Cambridge Ltd*, England was used. The energy of the electron beam was adjusted from 300 V to 30 KV in 10 V steps and the electron beam current was continuously adjustable from 1 pA to 1 μA to suit the type of examination in progress. The SEM micrographs were obtained for the free films of IPNs and other neat systems. The circular free film of respective test polymer with 1 cm diameter was mounted vertically on a SEM stub by silver adhesive paste. The specimen was coated with a thin layer of gold

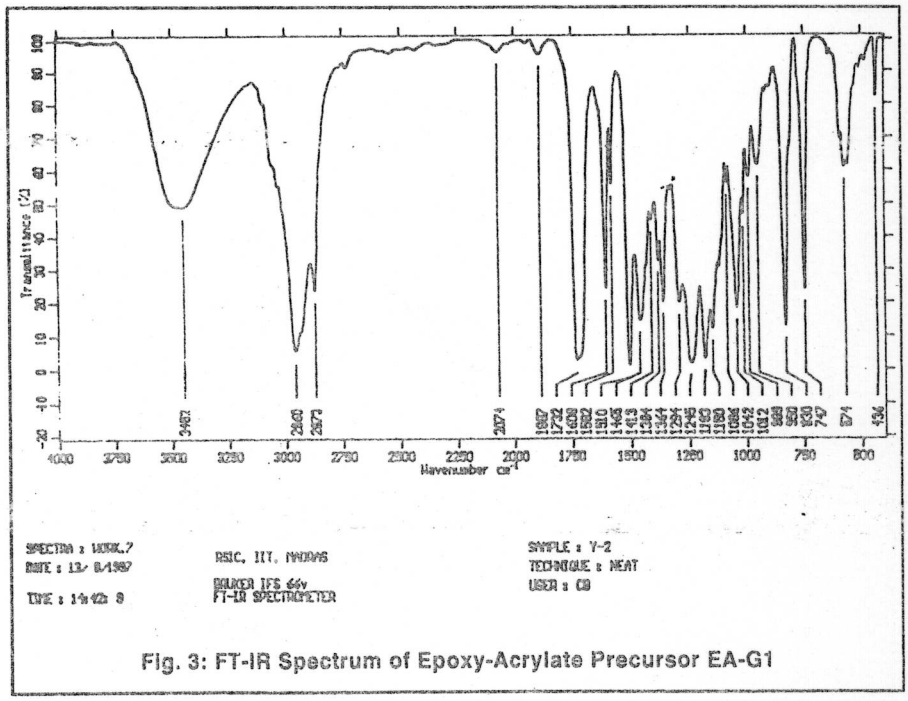

Fig. 3: FT-IR Spectrum of Epoxy-Acrylate Precursor EA-G1

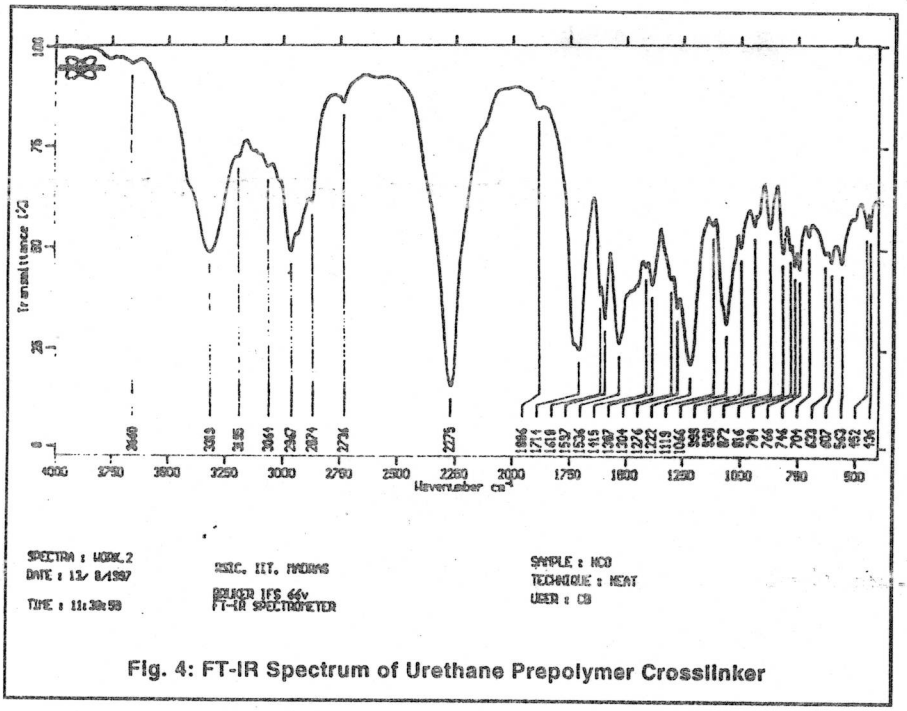

Fig. 4: FT-IR Spectrum of Urethane Prepolymer Crosslinker

(about 200 angstrom thickness) using a high vacuum gold sputterer (like the system EPS/Carl Zeiss) at about 10^{-4} to 10^{-6} torr and then scanned for surface properties.

Thermal measurements

For thermal measurements, *STA 1500 Simultaneous Thermal Analyser System* supplied by the Polymer Laboratories, UK was used. The entire system was software-controlled (V400) for data processing and analysis. The output data for the samples were fed into the computer through analog/digital converter in the form of mV. The thermo-gravimetric and differential thermal analysis curves were recorded simultaneously.

The samples in the form of fine powder of clear free films of all the coatings ranging from 4-8 mgm in weight (size) were placed in the platinum sample pans under a continuous nitrogen flow of 25 ml../minute (provided by a N_2 generator supplied by *Peak Scientific Company*, India). The sample and the reference (α-alumina) were heated at the rate of 10°C/minute.

The glass transition temperatures were measured on a *Perkin- Elmer Differential Scanning Calorimeter, DSC-2.* Measurements were carried out from -120°C to +120°C under helium at a scanning rate of 10°C/minute. Specimen sizes were in the order of 20 mgm.

Gel-time measurements

To study the gel time, one gram of each sample of clear coating material without pigments was poured into a glass tube (12 cm long, 8 mm dia.) and the tubes were sealed subsequently. These capsules were then placed in an oil bath at about 110°C. The samples were taken out at different time intervals and were quenched in a dry ice- acetone bath and examined for flowability. The time at which the polymerizing mass does not flow at room temperature was reported as 'Gel Time'.

Moisture vapor transmission rate measurements

The popular 'Payne Cup' was used for this test [16]. The free films of the coatings were cut to size and placed in between the cup and its lid. The bottom portion of the cup contained water. After the film was placed, the lid was placed and tightly sealed. The cup with the film and water was then weighed in an electronic balance to an accuracy of 1 mgm and placed in a desiccater containing a powerful desiccant, silica gel. After every 24 hrs., the cup was taken and weighed accurately. The loss of water was noted. After the loss per day reached a steady state, the MVT rate was calculated as loss of water in mgms./day/25 micron film thickness/ cm^2.

Electrochemical AC Impedance Spectroscopy (EIS)

For the electrochemical AC impedance spectroscopic studies an electrochemical impedance system of Model 6310 EC Electrochemical Impedance Analyzer supplied by the *EG & G Princeton Applied Research Corporation* was used.

The electrochemical test cell arrangement used [17-19] in this study is shown in *Figure-1*. The coated speci-

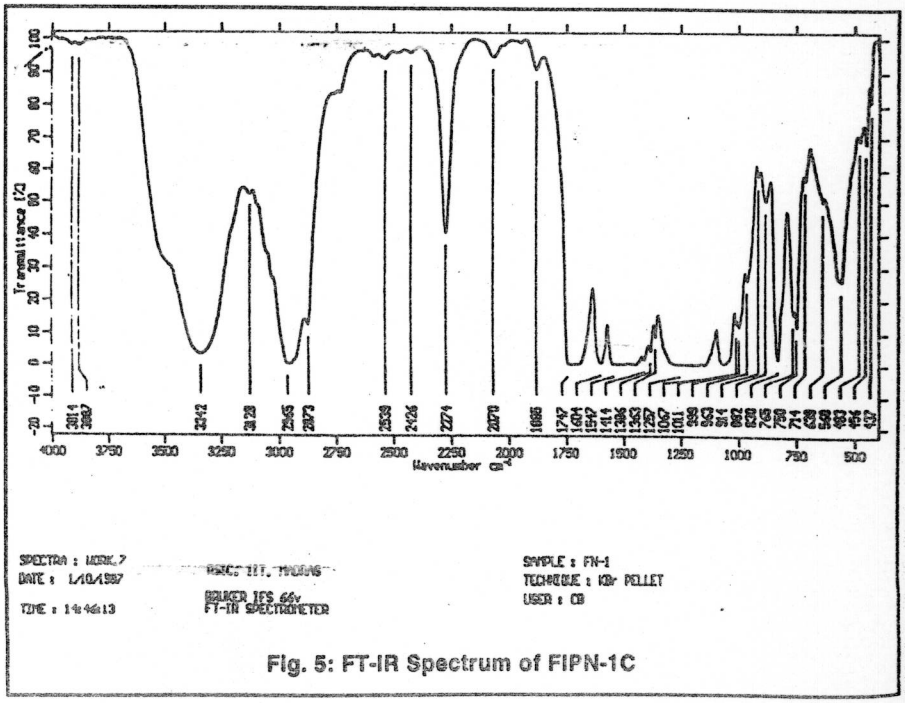

Fig. 5: FT-IR Spectrum of FIPN-1C

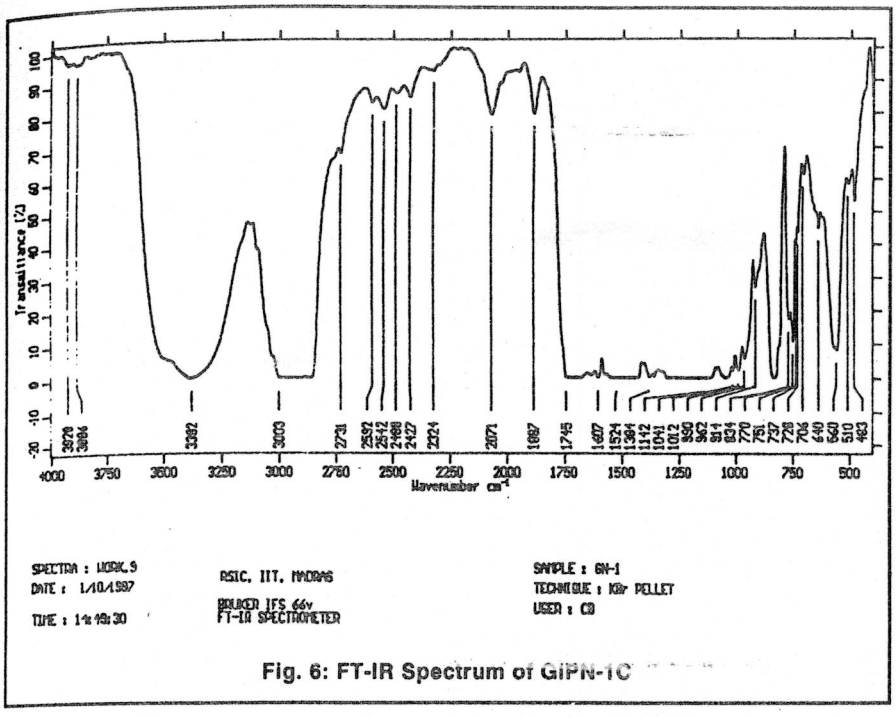

Fig. 6: FT-IR Spectrum of GIPN-1C

men was fixed with a glass tube vertically using an M-Seal type adhesive in which a 3% w/v aqueous NaCl solution as corrosive electrolyte was filled with ambient aeration. The area of the working electrode was 1 cm^2 in all cases. The electrochemical set-up was arranged in such a way that the coated metal was the working electrode, along with a reference electrode (saturated calomel electrode) and a counter electrode (platinum electrode). Impedance data were obtained over the range of 0.1 to 10,000 Hz at a small excitation amplitude of 10 mV peak to peak. The measurements were made at regular intervals at ambient conditions. The R_{po} and C_c were calculated and presented.

Results and discussion

FT-IR spectra

Figures 2 to *4* show the FT-IR spectra of each of the synthesized representative epoxy-acrylate precursors with urethane crosslinker and *Figures 5* to *5* show the FT-IR spectra of each of the representative IPN coatings.

The epoxy group shows three characteristic absorption bands. The region of the first band is small and it lies mostly at about 1250 cm^{-1}. The regions of the two other bands are broader, the position of the maximum depending on the structure of the epoxide. These absorption bands appear between 950- and 860 cm^{-1} (generally at 916cm^{-1}) and between 865 and 785 cm^{-1} (generally at 830 cm^{-1}) [20-22]. *Henbest et al.* proposed absorption bands at about 3000 cm^{-1} as a means of detecting epoxides [23]. These bands are due to stretching vibrations of CH and CH_2 groups contained in epoxide rings. Bands in the far-infrared region at 570 cm^{-1} and 370 cm^{-1} have also been reported by *Hummel* [24].

From the infrared spectra, it can be seen that the bands at 916 cm^{-1} and 863 cm^{-1} are also due to epoxy groups, the latter being overlapped by an out-of-plane vibration of hydrogen in the p-di substituted ring. A carbon-oxygen single bond stretching of phenyl ether overlaps the 1250 cm^{-1}-epoxide band. The phenyl absorbance is confirmed at 1582 cm^{-1}.

It can also be seen from the spectra of the IPN films (*Figures 17* to *22*) that the IPN polymers showed the characteristic polyurethane group frequencies indicating the formation of urethane linkages.

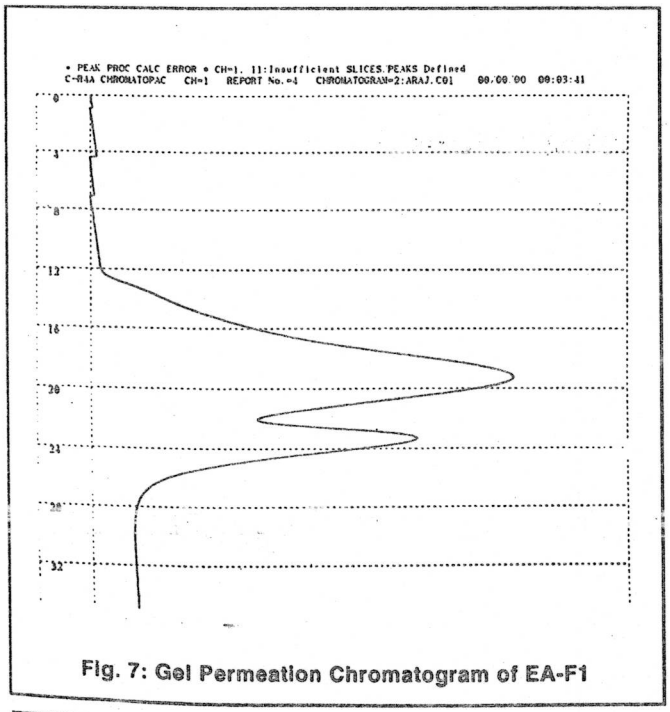

Fig. 7: Gel Permeation Chromatogram of EA-F1

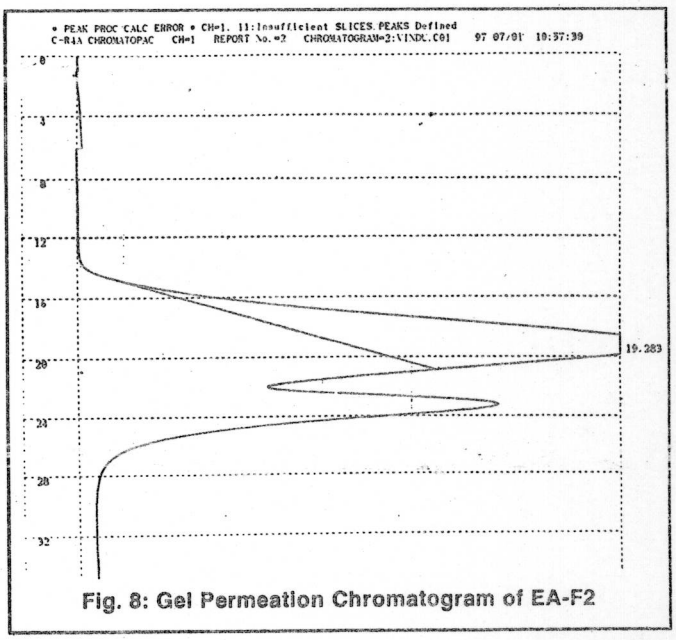

Fig. 8: Gel Permeation Chromatogram of EA-F2

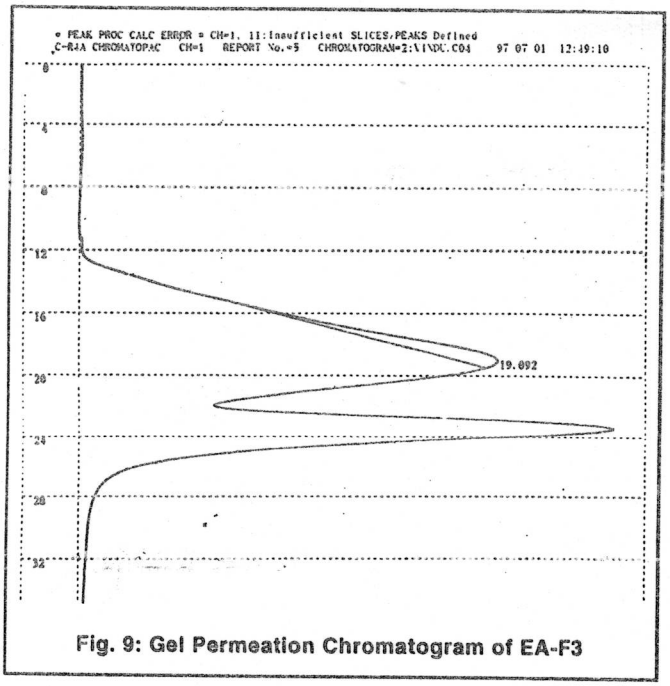

Fig. 9: Gel Permeation Chromatogram of EA-F3

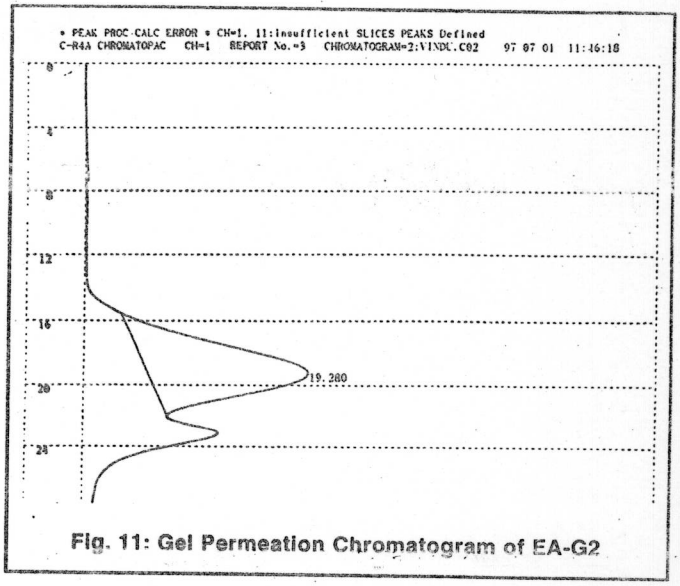

Fig. 11: Gel Permeation Chromatogram of EA-G2

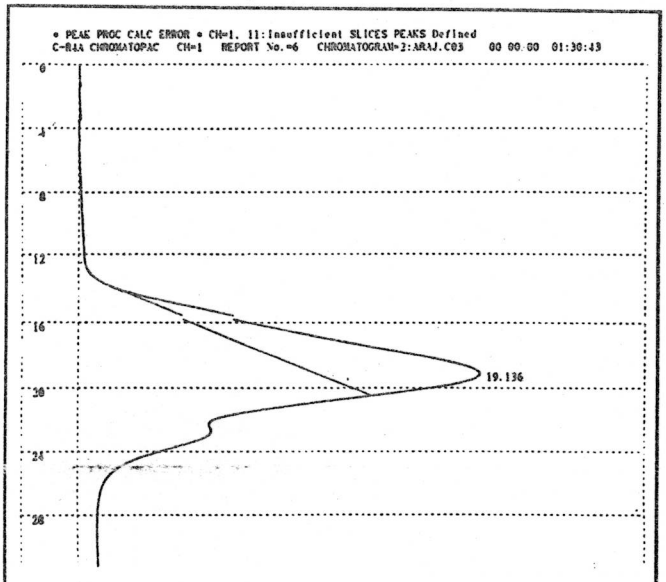

Fig. 10: Gel Permeation Chromatogram of EA-G1

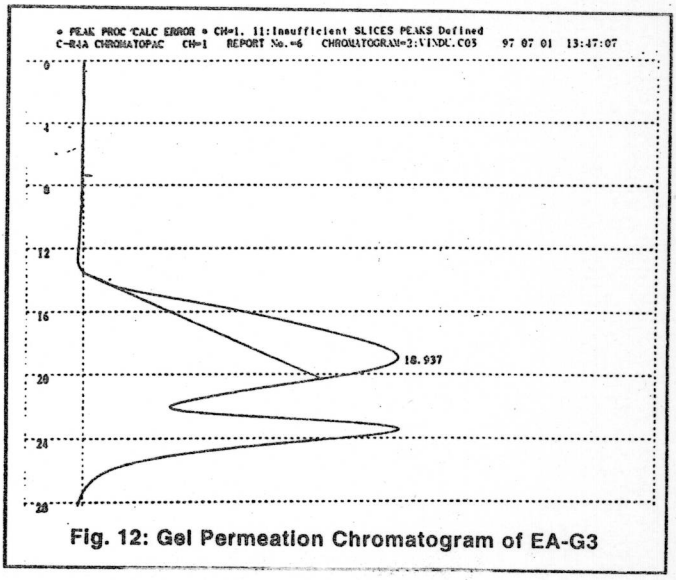

Fig. 12: Gel Permeation Chromatogram of EA-G3

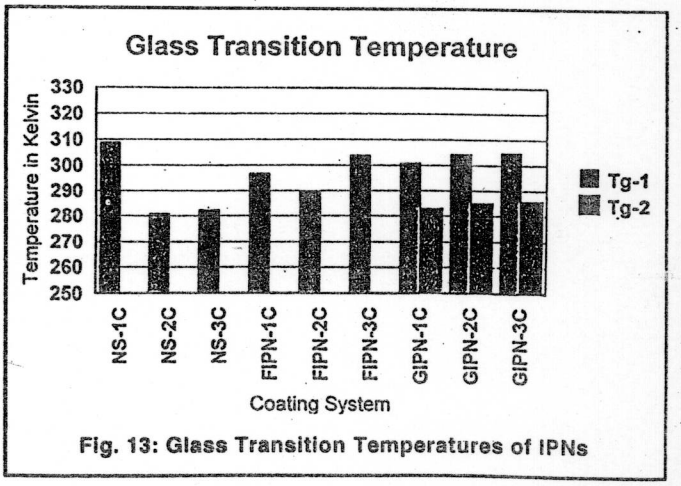

Fig. 13: Glass Transition Temperatures of IPNs

From the spectra, the isocyanate, NCO-, absorption band found at 2270 cm^{-1}, as the N=C=O stretching band, is confirmed. Appearance of band at about 1520 cm^{-1} and about 1740 cm^{-1} are due to the formation of urethane linkage. The band observed at 1242 cm^{-1} is due to the ester C=O of the solvent used in the system and is also used to monitor the solvent loss. The absorption at 1147 cm^{-1} confirms the presence of C-O-C band. The bands at 1420 and at 1710 cm^{-1} observed in a few samples may be due to the isocyanurate formed by a trimerisation reaction of isocyanate.

The IR spectra clearly indicate the presence of the reactive groups in the case of the precursors and in the fully cured films, and confirm the formation of urethane linkages.

Gel permeation chromatograms

Figures 7 to *12* depict the gel permeation chromatograms obtained for all the epoxy-acrylate precursors. The number average molecular weight and the polydispersity of the corresponding epoxy-acrylate precursors and the urethane crosslinkers obtained from the figures are summarized in *Table-2*.

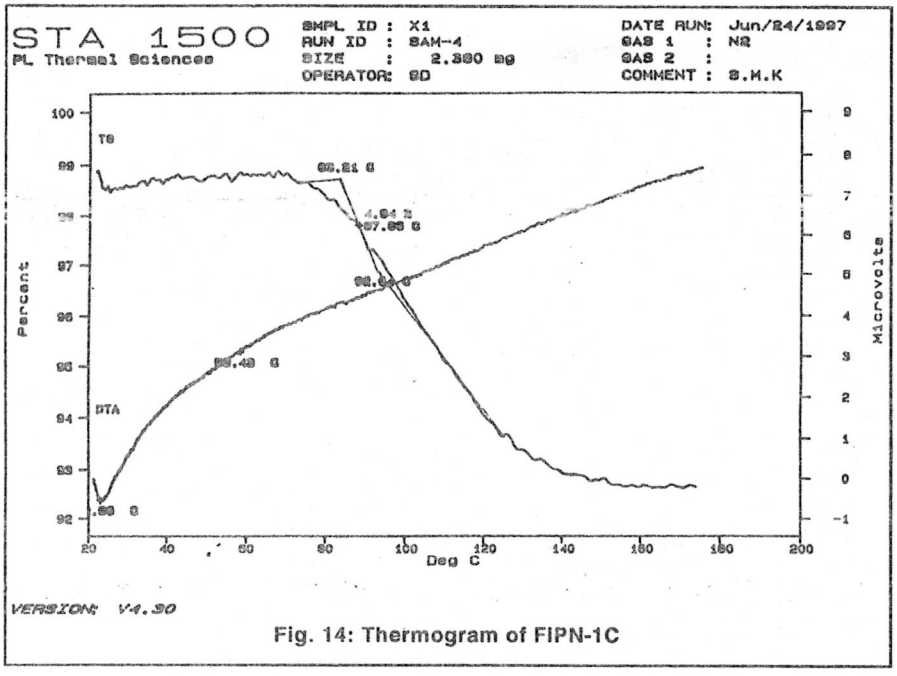

Fig. 14: Thermogram of FIPN-1C

TABLE 2: GEL PERMEATION CHROMATOGRAPHY

(Number and Weight Average Molecular Weights of Neat Polymers & Precursors)

System	Mn (g/mole)	Mw	Dispersity
EA-F1	6384	16222	2.541
EA-F2	5807	35372	2.762
EA-F3	12807	21829	1.704
EA-G1	9260	31197	3.364
EA-G2	4307	12866	2.986
EA-G3	12015	40548	3.375

From *Table-2*, it can be seen that the weight average molecular weights of all the synthesized samples are greater than the number average molecular weights, indicating that the synthesized polymers are inhomogeneous [25]. (Homogeneity in molecular sizes where Mw = Mn can not happen in the case of synthetic polymers.). The polydispersities of the synthesized polymers using the free-radical polymerization are well within the limits, indicating the synthetic procedures with optimum conditions [26-27].

Thermal measurements

From the glass transition temperature measurements (*Table-3* and *Figure-13*) obtained by differential scanning calorimetric analysis, it was found that the full-IPN based coatings with varying amounts of epoxy-urethane / crosslinked acrylic polymer exhibited only one Tg value, which was between the Tgs of the component polymeric systems [28-29].

TABLE 3:
Tg VALUES OF POLYMERS (IN °K)

System	Tg (°K)	
NS-1C	309	
NS-2C	281	
NS-3C	282.5	
FIPN-1C	297	
FIPN-2C	290	
FIPN-3C	304	
GIPN-1C	301	282.6
GIPN-2C	304.5	284.7
GIPN-3C	305	285.5

This implies that the formation of interpenetration between epoxy-urethane/ crosslinked acrylic polymer components were by complete segmental mixing resulting in a single glass transition temperature. As a result, NS-1 with high crosslink density (due to the many double bonds in the side chain) and rigid acrylic structure gave high Tg values and the NS-2 and NS-3 with relatively high crosslink density but with more and flexible urethane elastomeric structure gave low Tg values. The Tg values of IPN coatings shifted inwardly towards the direction of the NS-2 and NS-3 with increasing concentration of epoxy and urethane.

In the case of grafted-IPNs, two distinct Tgs for each composition that were also between the Tgs of the component polymers were obtained. This type of behavior has been noticed by many authors. These results imply that phase separation had occurred to some extent in grafted-IPNs due to the fact that the free energy of mixing in the systems may be either positive or zero because of the lack of any kind of physical interactions between the polymer components and also due to the grafting induced, whereupon partially newer covalent bonds are formed between

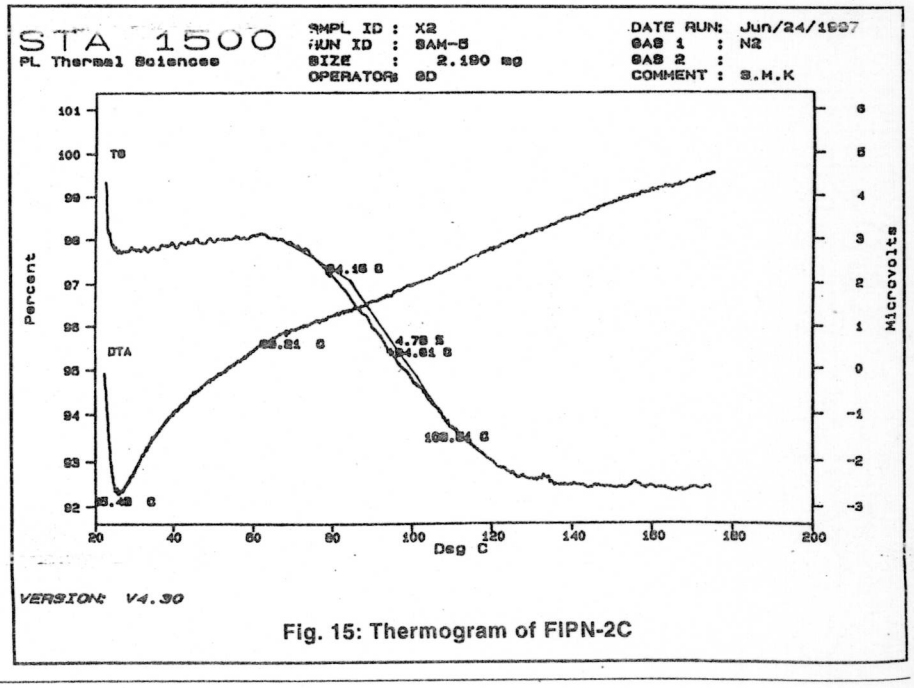

Fig. 15: Thermogram of FIPN-2C

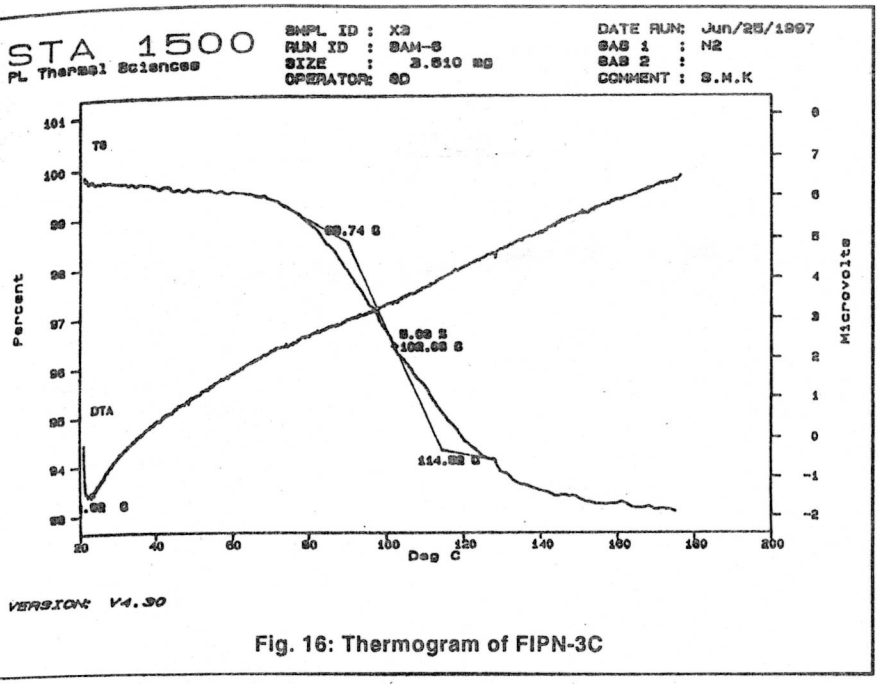

Fig. 16: Thermogram of FIPN-3C

TABLE 4: CHARACTERISTIC THERMAL DATA

System	Decomposition Range (°C)			% Wt. Loss (±2%) upto various temperatures		
	First[1]	Second[2]	Third[3]	80°C	100°C	120°C
FIPN-1C	83.21	87.66	92.64	1.8	4.2	7.0
FIPN-2C	84.16	94.61	108.54	3.1	5.0	6.8
FIPN-3C	89.74	101.25	114.0	1.1	3.6	5.3
GIPN-1C	89.40	101.25	114.0	1.0	3.5	5.9
GIPN-2C	81.86	99.91	113.41	0.9	3.6	5.6
GIPN-3C	76.7	96.98	114.74	0.8	3.0	4.8

1. Weight Loss due to retained moisture *2. Major decomposition stage*
3. Secondary decomposition stage

the component polymers within the networks.

The results of the thermo-analysis by TGA and DTA of full- and grafted-IPNs are shown in *Figures 14* to *19*. The IPNs exhibit higher weight retention compared to the weight retention of the neat systems NS-1C, NS-2C and NS-3C.

The TGA and DTA thermograms of all the IPNs presented in the figures give a comparative picture regarding the thermal stability of the IPNs. The characteristic thermal data are presented in *Table-4* along with the weight loss at different temperature ranges. A cursory glance at the table and figures shows that all the IPNs under study decompose in different distinct temperature ranges [30-31].

The initial slow weight loss around 50-55°C is attributed to moisture retained in the sample. In a few cases, there is a slight increase in the weight, which may be explained as the thermal expansion of the segments in the networks. The second weight loss occurs between 60-70°C in all IPNs, possibly due to decomposition of the acrylic polymers in the network forming free radicals. The third weight loss occurs during the range of 100-120°C, indicating the decrosslinking of the IPNs as well as further decomposition. The third weight loss for the full-IPNs lies between 100-110°C and for the grafted-IPNs; it is between 110-120°C (around 114°C) showing that the covalent bonds due to the grafting occurring within the networks. These covalent bonds decrosslink at higher temperatures than the full-IPNs, in which such graftings were almost absent.

As the weight loss in all the IPNs is not uniform to show any systematic trend of thermal stability in the series, it is difficult to arrive at any conclusion regarding the structural variations in the IPNs, except the usual decrosslinking phases. In DTA measurements, it can be observed that in the case of full-IPNs, an endothermic peak is observed, whereas this peak is almost absent in the cases of grafted-IPNs.

The comparison between the full- and grafted-IPNs indicates that there

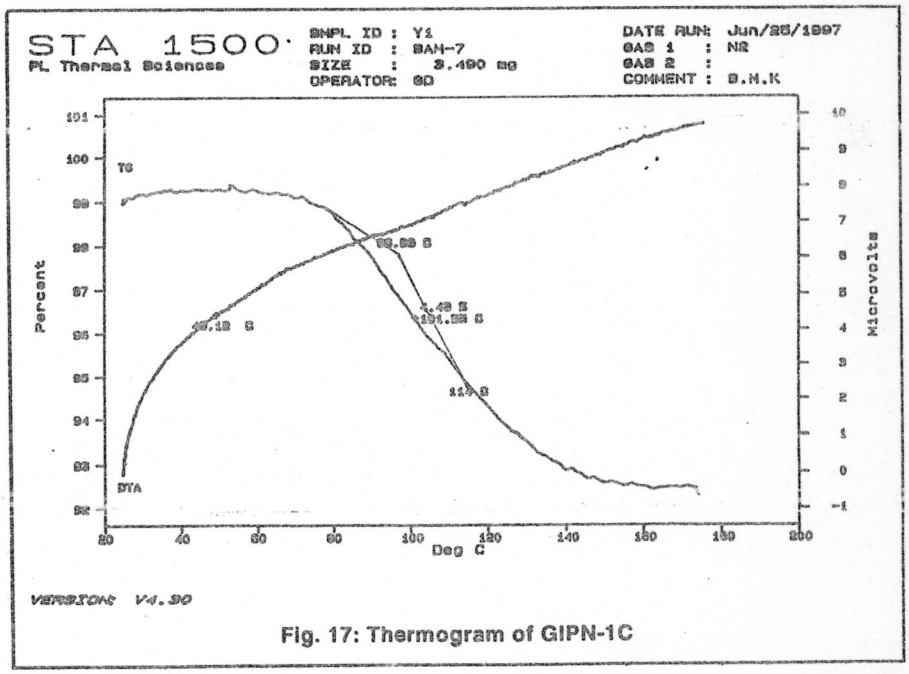

Fig. 17: Thermogram of GIPN-1C

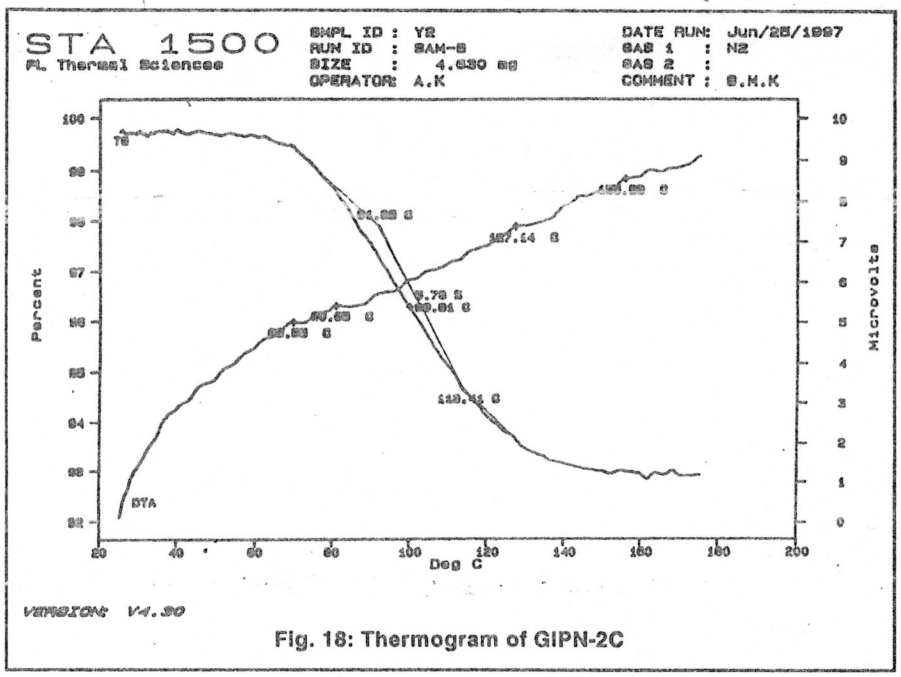

Fig. 18: Thermogram of GIPN-2C

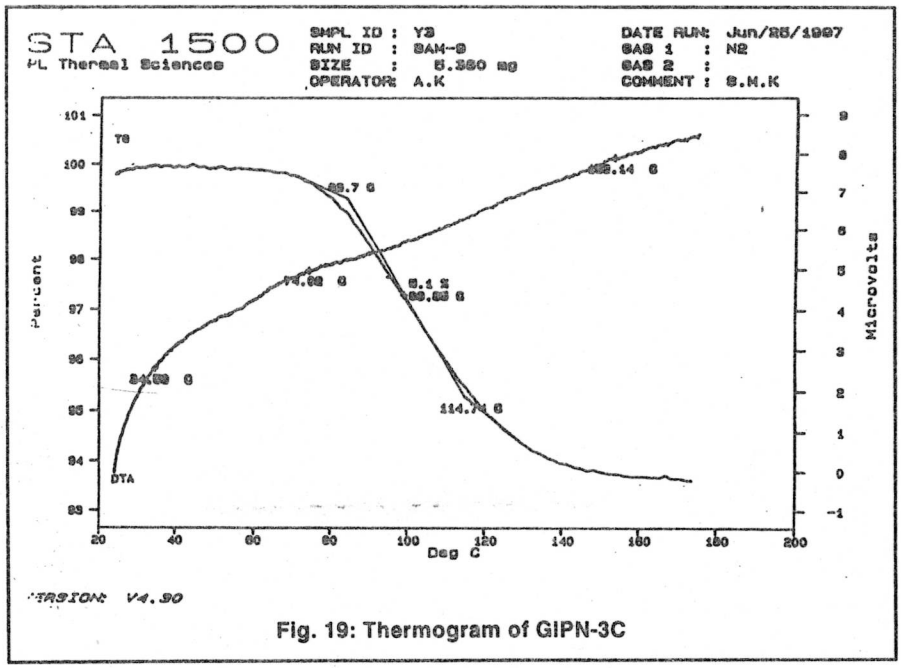

Fig. 19: Thermogram of GIPN-3C

is no significant difference in the degradation behaviour and that the enhancement is not related to the interpenetration. The higher weight retention of the IPNs can be explained by the fact that the thermal degradation behaviour of crosslinked acrylic polymer in the polymer alloys is known to yield almost 100% monomer by stepwise unzipping process, and the unzipped monomers act as radical scavengers for the radicals produced from the degradation of epoxy-urethane, thus delaying further reaction of radical into thermo-degradative products of epoxy and urethane [32]. Thus the degree of intermixing of epoxy-urethane with crosslinked acrylic polymer networks may play an important role in the enhancement of thermal stability of the IPNs.

Morphology of IPNs by SEM

Micrographs obtained from the SEM provide vital information about not only the surface characteristics, but also information about the networks with the phase domains sizes. SEM Micrographs as *Figures 20* to *31*, show that the various IPN compositions exhibit only one phase at a magnification of roughly 1000x and 10 Kx. The presence of only one phase is indicative of good molecular mixing due to interpenetration between the component networks [33-36].

No visible white particles are seen in the dark urethane matrix. It is possible that in the absence of covalent bond formation, the network formation might have provided a better opportunity for interpenetration between the network of epoxy-urethane and acrylate.

As the dispersion of the white epoxy-polyurethane particles in the dark acrylate matrix is observed and also since no phase domain between the networks could be detected in the full-IPNs, it is concluded that interpenetration has occurred between the two polymer networks.

From the SEM micrographs of the full-IPNs (*Figures-20* to *25*), it can also be seen that full-IPNs with different compositions exhibit only one phase at a magnification of about 1000x. It can also be seen that some small particles of the epoxy-polyurethane dispersed in the dark acrylic matrix. The size of the small particles may be in the range of 10 to 100 angstrom, indicating the molecular mixing resulting from interpenetration between the networks having finer to intermediate structures. From the micrographs, an improvement in molecular mixing can be seen because of the permanent interpenetration of the two networks [34-36].

TABLE 5:
GEL-TIME AND MVT RATES MEASUREMENTS

System	Gel Time (Mins)	MVTR (mgms/cm²/day/25μm)
NS-1P	13.5	---
NS-2P	8.1	5.45
NS-3P	7.6	5.15
FIPN-1P	5.6	4.0
FIPN-2P	5.9	4.15
FIPN-3P	6.5	4.0
GIPN-1P	5.8	4.15
GIPN-2P	6.1	4.15
GIPN-3P	7.1	4.15

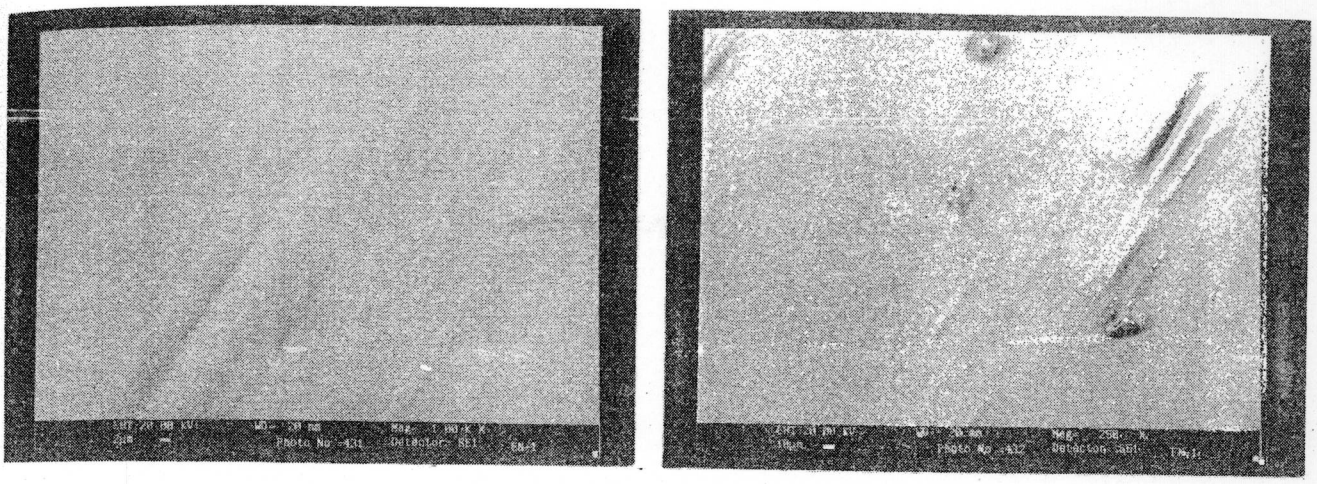

Fig. 20 & 21: SEM Micrographs of FIPN-1C

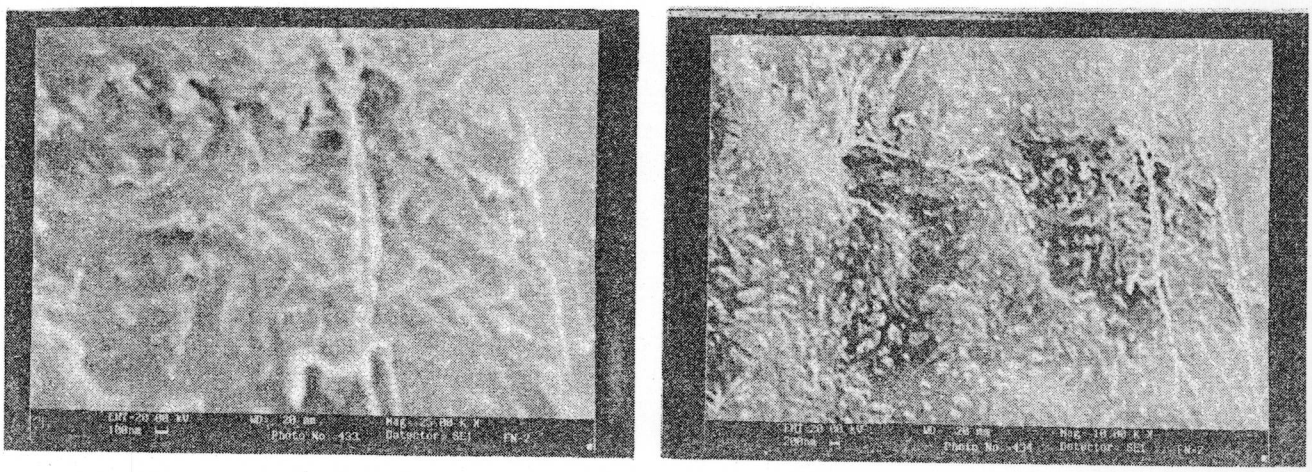

Fig. 22 & 23: SEM Micrographs of FIPN-2C

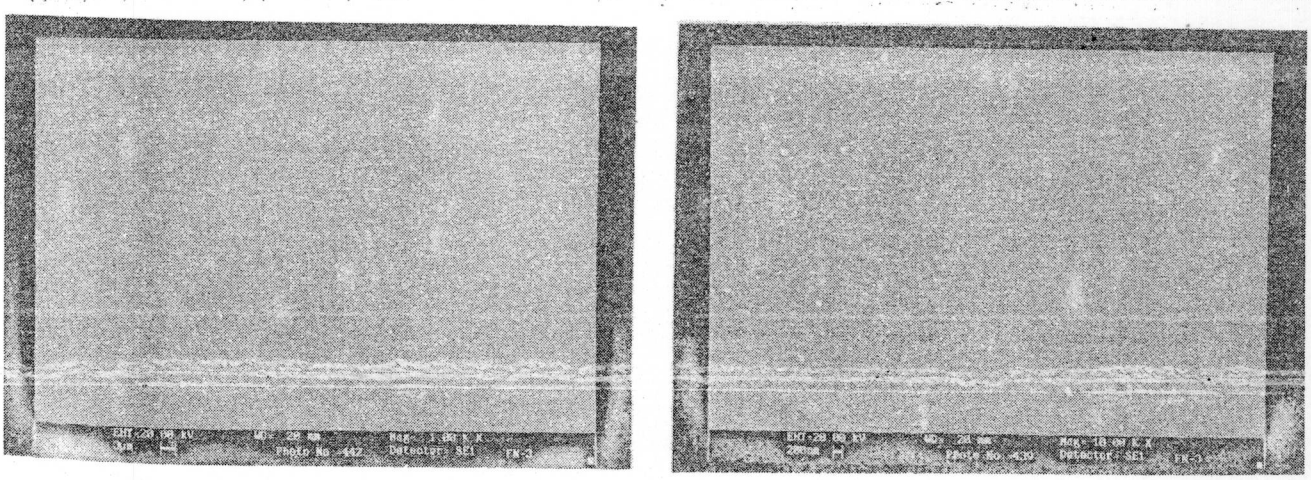

Fig. 24 & 25: SEM Micrographs of FIPN-3C

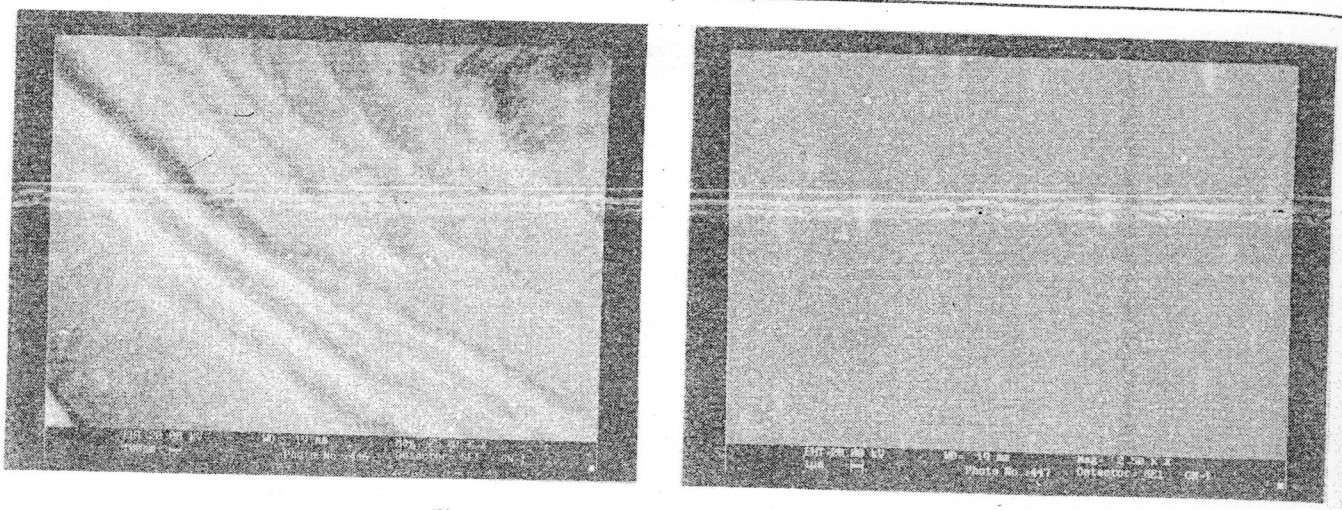

Fig. 26 & 27: SEM Micrographs of GIPN-1C

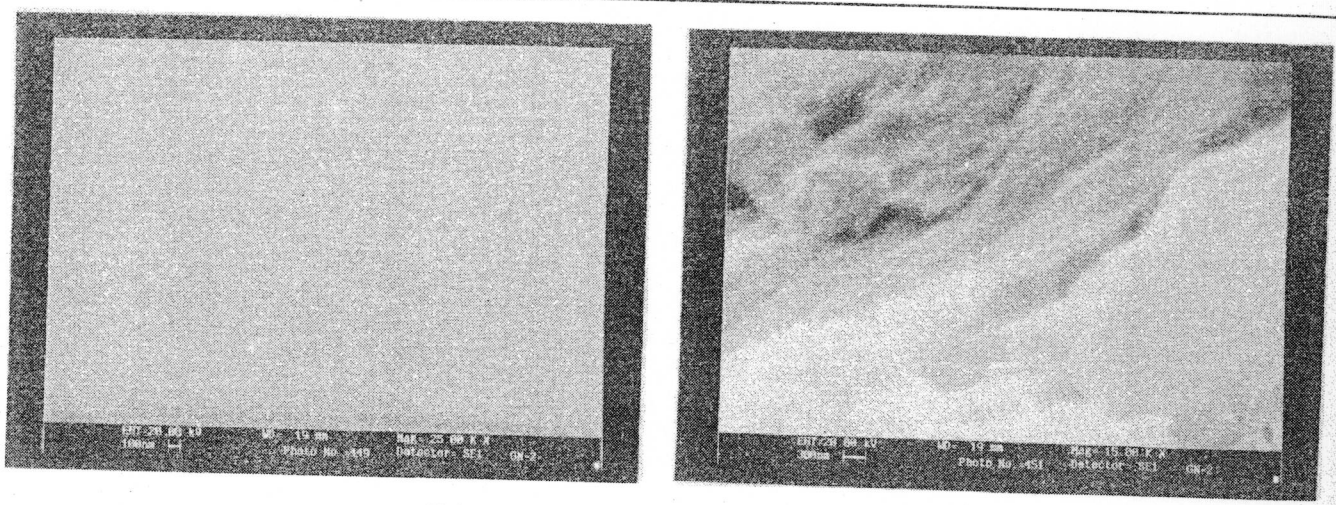

Fig. 28 & 29: SEM Micrographs of GIPN-2C

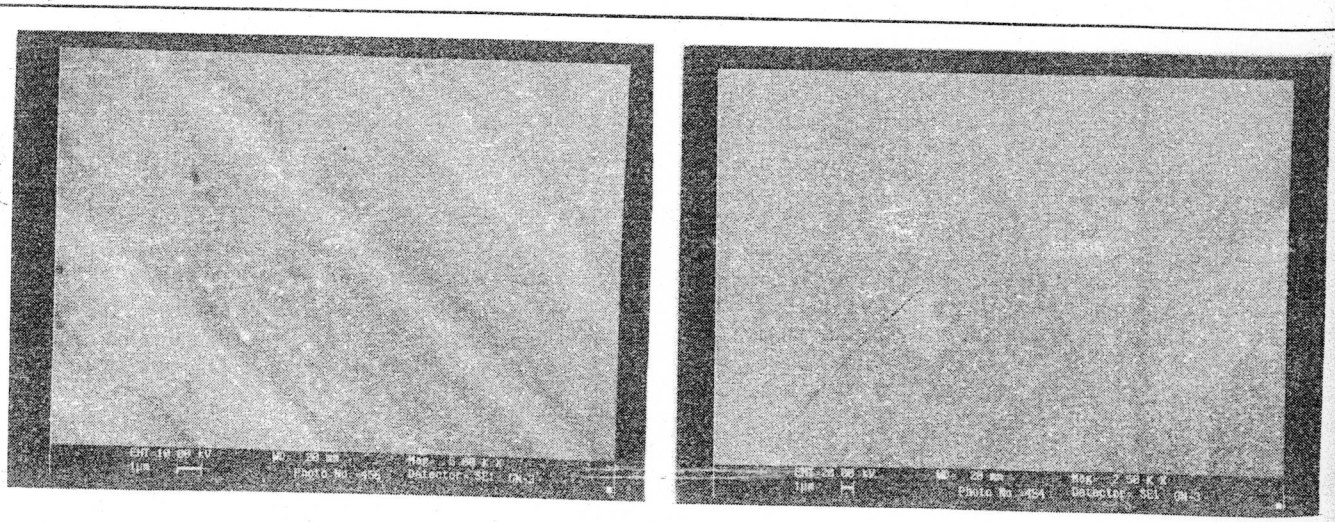

Fig. 30 & 31: SEM Micrographs of GIPN-3C

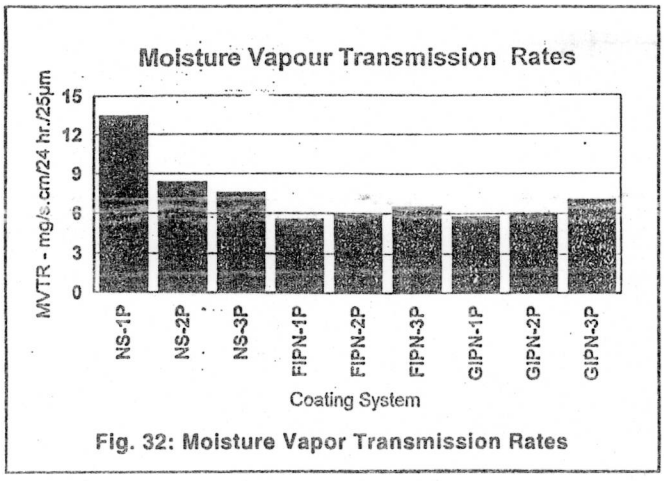

Fig. 32: Moisture Vapor Transmission Rates

While the acrylate network is present initially and the interpenetration of epoxy-polyurethane component occurs during the IPN synthesis, the acrylate is a continuous phase in which the second component epoxy-polyurethane is entangled. SEM micrographs of the grafted-IPNs (*Figures-26* to *31*) show that there are two distinct phase domains due to phase separation of the two component networks and they exhibit obvious phase separation in which the white epoxy-polyurethane particles are dispersed in the dark matrix of the acrylate polymer.

Epoxy-polyurethane, with an average phase domain size 100 nm, is dispersed throughout the acrylate matrix. The boundaries between the matrix and the epoxy-polyurethane phase inclusion seem to be clear and distinct. However, an enlargement of these boundaries reveals gray regions that are not well defined and may be due to an enlargement of epoxy-polyurethane network within the acrylate, resulting in a minimal degree of mixing [35-36].

Increasing the concentration of epoxy-polyurethane content, the area of dispersed phase of epoxy-polyurethane polymer was increased with the epoxy-polyurethane particles in close proximity to each other. However, the minimal degree of molecular mixing observed in the case of these IPNs is due to the covalent bonding between the two networks, which makes the graft a semi-rigid structure with an improved morphology over the other polymer blends [34-35].

Gel-time measurements

Gel-time measurements form an important aspect of IPNs as they decide the optimum conditions of curing and obtaining reasonable pot life. The results of the gel-time measurements are shown in *Table-5*. These results were employed for manipulating the optimum concentration of the catalyst and NCO/OH ratio for forming films of full- and grafted-IPNs satisfactorily at ambient conditions without any film defects. In this study, the NCO/OH ratio of 1.05 was found to be highly suitable to provide the required film properties in equivalent ratios.

Moisture-vapor transmission rates

The MVT rates shown in *Table-5* and *Figure-32* are true reflections of the permeability of all coatings. The neat system NS-1P gives the highest MVT rates indicating its pervious nature leading to poor corrosion resistance [37-40]. This may be attributed to the possible dissolution (wash off) of the low molecular weight fractions of the crosslinked acrylic polymer and to the presence of any inclusion of solvent trapping due to its faster drying time. The full- and grafted-IPNs have shown appreciably lower MVT rates than the other neat systems like NS-2P and NS-3P, indicating the superior protective merits. Full-IPNs have shown lower rates than the grafted-IPNs. However, the difference between them is not much. This is due to the difference in crosslink densities between the two chains. The FIPN-1P & 2P and GIPN-1P & 2P series have

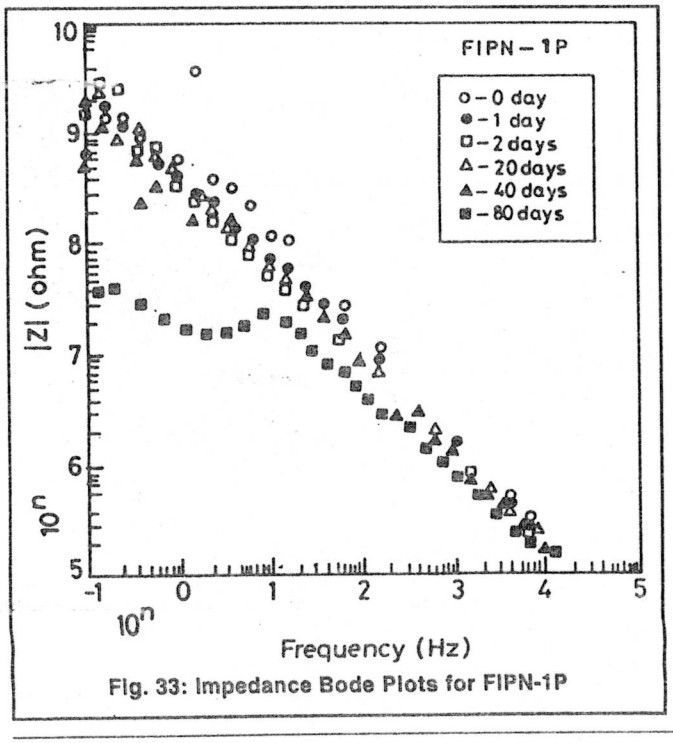

Fig. 33: Impedance Bode Plots for FIPN-1P

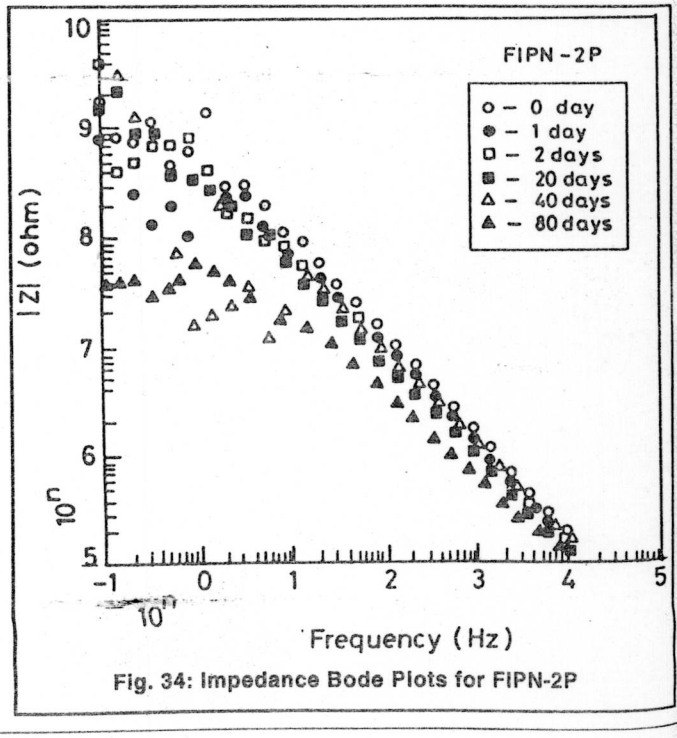

Fig. 34: Impedance Bode Plots for FIPN-2P

shown lower rates among the various IPN ratios, probably due to the higher epoxy-urethane content present in the respective IPNs.

It can also be seen from the MVT rates, that the IPNs with lower rates can be effective corrosion resistant materials, as the interlocking of the polymer segments inhibits the process of permeation.

Electrochemical AC impedance spectroscopy

From the electrochemical AC impedance responses of the painted steel electrodes in 3% NACl solution, the variations of R_{po} and C_c have been calculated and the results are presented in *Table-6*.

AC impedance spectroscopic responses, obtained from all the painted electrodes after various periods (viz., 0,1,2,20,40 & 80 days) of immersion in the NaCl electrolyte are shown in *Figures-33* to *38*. From the figures, it can be seen that the high frequency part of each curve in all systems exhibits a linear increase of log /Z/ Vs. log f values. The log /Z/ is invariant with frequency which is an indicative of the response of a pure resistor. Overall, the plots can be considered representative of the response owing to the coating and can be modeled in terms of simple, parallel, resistance-capacitance (RC) equivalent electrical circuits [41-43].

It may be seen from Table-6 that the resistance of the various types of the coatings initially lies above 10^8 Ω cm². In the case of NS-1P system, there is a gradual decrease in resistance with time, which achieves a value of 10^6 Ω cm², corresponding to the condition of failure. In all the other systems, the resistance values lie above 10^8 Ω cm² even after 80 days of exposure.

From the impedance data, it is also possible to calculate capacitance value according to the following relationship:

$$C_p = 1 / (2 \pi f Z'')$$

where Z" is the imaginary component of impedance in a region of the spectrum when Z" ~ Z and Z" α 1/f.

Increasing capacitance value is indicative of an increased water uptake (electrolyte), leading to the onset of corrosion at the interface.

In practice, as the coatings degrade, the coating capacitance increases and the paint film resistance decreases due to the transport of electrolyte through the coating to the metal substrate and the formation of ionically conducting paths (pores).

From *Table-6*, it can also be seen that the capacitance of the FIPN and GIPN series has initially shown lower values and as exposure time increases, an increased capacitance value is obtained. Almost in all cases of FIPNs and GIPNs, the capacitance values have shown a gradual decrease (except a few anomalies) indicating the formation of pores in the coating and leading to the passage of electrolytes through the film [43-45].

Conclusions

1. The results convincingly brought out that the full-IPNs and the grafted-IPNs synthesized from the homopolymers of polyurethane, epoxy and acrylics had far superior properties when compared to their constituent-polymers and

TABLE 6: VARIATIONS OF R_{po} AND C_c IN PAINTED STEEL ELECTRODES

System	Exposure Period (in days)	R_{po} (Ohms)	C_c (Farad / cm²)
NS-1C	0	6.4×10^8	5.0×10^{-12}
	1	1.2×10^9	2.0×10^{-11}
	2	4.8×10^9	5.0×10^{-11}
	20	2.8×10^8	5.0×10^{-12}
	40	7.6×10^7	2.5×10^{-11}
	80	1.9×10^6	1.0×10^{-7}
NS-2C	0	2.1×10^8	5.0×10^{-12}
	1	1.8×10^8	1.11×10^{-11}
	2	8.1×10^8	1.11×10^{-11}
	20	1.5×10^9	1.25×10^{-11}
	40	1.2×10^9	1.43×10^{-11}
	80	9.0×10^8	1.43×10^{-11}
NS-3C	0	3.1×10^8	1.25×10^{-11}
	1	4.1×10^8	1.25×10^{-11}
	2	6.0×10^8	1.43×10^{-11}
	20	1.5×10^9	2.0×10^{-11}
	40	1.5×10^9	1.25×10^{-11}
	80	1.5×10^9	2.00×10^{-11}
FIPN-1C	0	7.0×10^8	3.33×10^{-12}
	1	1.5×10^9	1.11×10^{-11}
	2	1.5×10^9	1.67×10^{-11}
	20	2.6×10^9	1.43×10^{-11}
	40	5.0×10^8	1.43×10^{-11}
	80	2.0×10^8	1.25×10^{-10}
FIPN-2C	0	8.0×10^8	5.0×10^{-12}
	1	8.5×10^9	1.11×10^{-11}
	2	5.0×10^9	1.11×10^{-11}
	20	1.0×10^9	1.25×10^{-11}
	40	9.0×10^9	1.25×10^{-11}
	80	7.0×10^8	1.11×10^{-10}
FIPN-3C	0	9.0×10^8	6.67×10^{-12}
	1	4.0×10^8	3.33×10^{-12}
	2	4.0×10^9	1.11×10^{-11}
	20	5.2×10^9	1.11×10^{-11}
	40	5.0×10^9	1.25×10^{-11}
	80	7.0×10^8	1.43×10^{-11}
GIPN-1C	0	8.0×10^8	3.33×10^{-12}
	1	7.0×10^8	1.00×10^{-11}
	2	1.5×10^9	1.11×10^{-11}
	20	9.0×10^8	1.67×10^{-11}
	40	9.0×10^8	2.50×10^{-11}
	80	2.5×10^8	5.0×10^{-11}
GIPN-2C	0	1.5×10^9	1.0×10^{-11}
	1	1.5×10^9	5.0×10^{-12}
	2	2.5×10^9	1.0×10^{-11}
	20	1.5×10^{10}	1.0×10^{-11}
	40	6.0×10^8	1.11×10^{-11}
	80	3.0×10^9	2.0×10^{-10}
GIPN-3C	0	7.0×10^8	5.0×10^{-10}
	1	1.5×10^9	1.25×10^{-11}
	2	1.0×10^9	1.25×10^{-11}
	20	2.5×10^9	1.25×10^{-11}
	40	7.0×10^9	1.11×10^{-11}
	80	5.0×10^8	1.67×10^{-11}

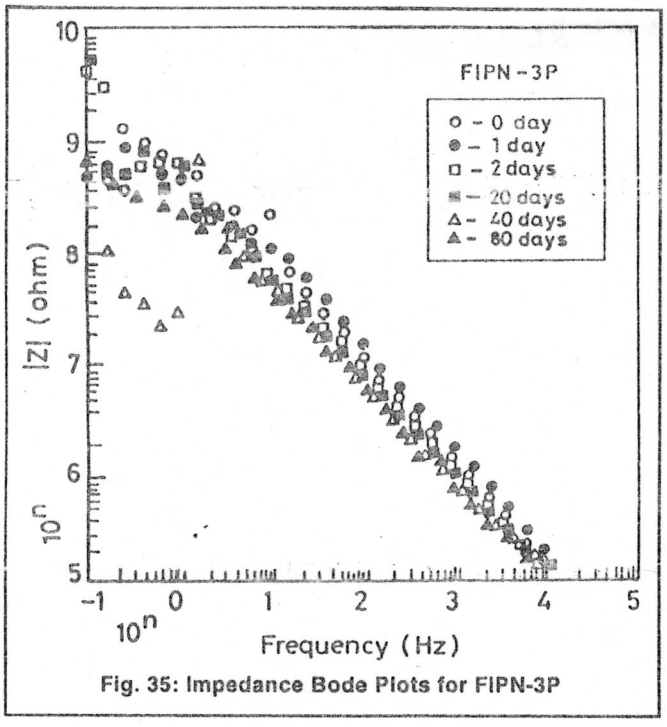

Fig. 35: Impedance Bode Plots for FIPN-3P

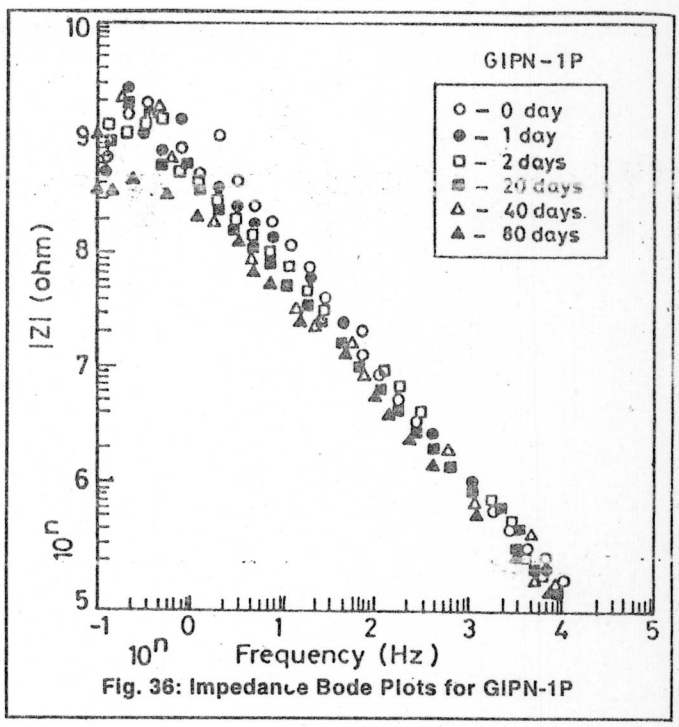

Fig. 36: Impedance Bode Plots for GIPN-1P

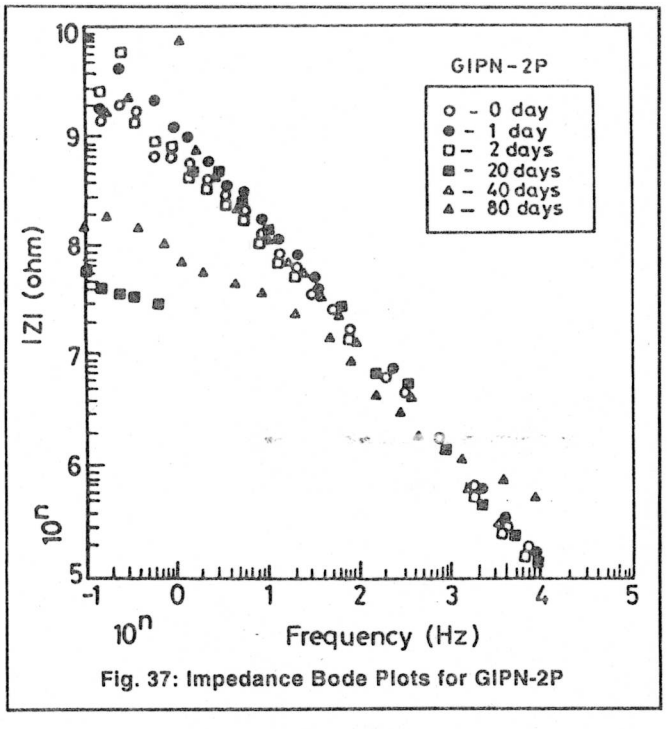

Fig. 37: Impedance Bode Plots for GIPN-2P

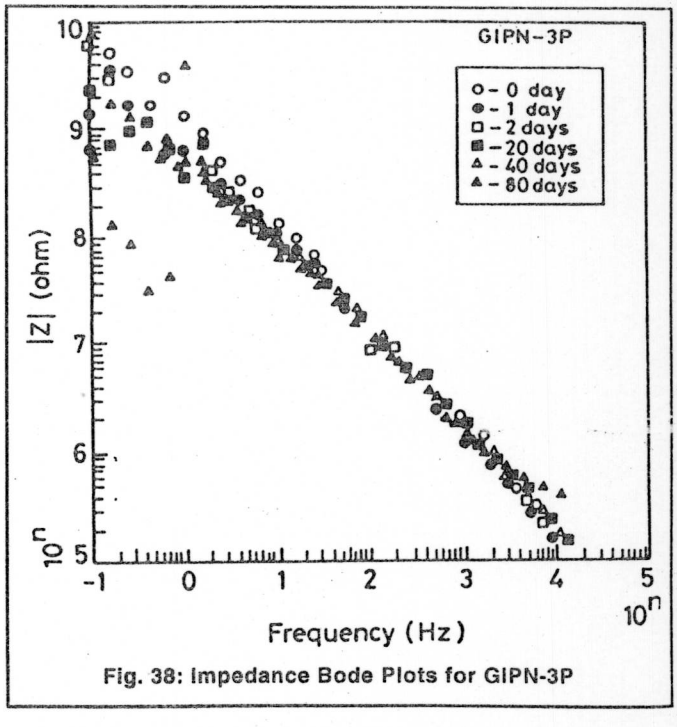

Fig. 38: Impedance Bode Plots for GIPN-3P

that they formed excellent vehicles for the preparation of organic coatings for corrosion protection in aggressive environments.

2. The SEM studies show the IPNs have morphological properties reflecting good molecular mixing among the components. Their phase domain sizes are so fine in the case of the full-IPNs that separate phases are not observed even under 10,000 x magnification.
3. In the thermal analysis of the IPNs, only one glass transition temperature is observed in the case of Full-IPNs, confirming the good interpenetration (molecular mixing) and absence of separate phases, whereas two transition temperatures are observed in the case of Grafted-IPNs, indicating the presence of two distinct phases.
4. AC impedance measurements also indicated that the coating impedance remains above 10^8 ohm-cm^2 during the period of test, which confirms the excellent condition of the coating throughout the testing period.
5. The present study has, thus, led to the development of polymer alloys based on full- and grafted-IPNs with good physical properties and excellent corrosion resistance properties. They have the promise of becoming good candidates for coat-

ings in highly corrosive environments with long-standing performance. The results of other laboratory accelerated tests such as salt spray, humidity, immersion in different media, accelerated weathering test, etc. conducted by the authors on these polymer alloy pigmented coatings also confirm this conclusion.

Acknowledgements

The authors of this paper would like to express their sincere thanks to Director, CECRI for permitting this work to be carried out at the laboratory and to the staff of Characterization & Instrumentation Laboratory, Thermo-Gravimetric Analysis, Electrochemical Impedance Spectroscopy and Glass Blowing Section.

References

1. Leszek.A.Utraki, *Polymer Alloys & Blends, Thermodynamics & Rheology,* Hanser Publishers, Munchen, 1987
2. L.H.Sperling, *Interpenetrating Polymer Networks and related materials,* Plenum Press, USA (1981)
3. D.Klempner, H.L.Frisch, et.al., *J.Polym.Sci.,* A-2, 8, 921 (1970)
4. L.H.Sperling et.al., *J.Polym.Sci.,* A-2, 7, 425, (1960)
5. L.H.Sperling et.al., *J.Polym.Sci.,* B-8, 525, (1970)
6. L.H.Sperling et.al., *J.Polym.Sci.,* 14, 2815 (1970)
7. P.F.Bruins, *Polymer Blends and Composites,* Wiley Interscience, NY, (1970)
8. KC Frisch et.al, *Polym.Engg.Sci.,* 14, 76, (1974)
9. HL Frisch et.al., *J.Am.Chem. Soc.,* 83, 3789, (1961)
10. HL Frisch et.al., *Adv.Macromol.Chem.,* 2, 149, (1970)
11. LH Sperling *'Recent Advances in Polymer Blends, grafts & block'* Plenum Press (1974)
12. MJD Low et.al., *J.Paint.Tech.,* 42,235 (1970)
13. MJD Low et.al., *J.Paint.Tech.,* 43,31,(1971)
14. MJD Low et.al., *J.Paint.Tech.,* 44,52 (1972)
15. Mir Mandik, *Prog.Org.Coat.,* 5,131-198 (1977)
16. HF Payne & WH Gardner, *Ind. Eng. Chem.,* 29, 893 (1937)
17. J Hobrecht et.al., *J.Electro.Chem.Soc,* 13, No.9 2010-15 (1924)
18. H Jr Leidheiser , *Prog.Org.Coat.* 7, 79 - 104 (1979)
19. F Mansfield et.al., *Corrosion,* 38,9,478-485 (1982)
20. G.Herzberg, *IR Raman spectra,* Vas Nostrand, Ny, P346,1945
21. J.E.Field et al, *J.Chem Soc.,* 18,1298,(1950)
22. J.Bomstein, *Anal.Chem.,* 30,544, (1958)
23. H.B. Hembest et.al., *J.Chem.Soc.,* 80,1459,(1957)
24. H.Lee. JK.Neville, *Handbook of Epoxy Resins,* McGraw Hill. Book Com., New York,(1967)
25. Mir Mandik, *Prog.Org.Coat.,* 5,131-198 (1977)
26. J.Brandrup. & EH Immergot, *Polymer Handbook,* 2nd Edi., Wiley, New York. 1975.
27. Seymour R.B. , & CE Carrahev,Jr, *Polymer Chemistry, An Introduction,* 2nd Edi., Dekker, New York,1987.
28. N. Devia et al, *Macromolecules,* 12,360, (1979)
29. LH Freling et al *J.Polym.Mater.,* 1, 54, (1984)
30. Turi(Editor), *Thermal Characterisation of Polymeric materials,* Academic, Orland,FL, (1981)
31. Robert.F.Speyer, *Thermal Analysis of Materials,* Marcel.Dekker, Inc, NewYork, (1994).
32. S.L. Madorsky, *"Thermal Segregation of organic polymers"* InterScience, New York, (1964).
33. D.Klempner et.al., *Polym.Engg.Sci.,* 10, 327, (1970)
34. Volker Huelck et al., *Macromolecules,* 5, 340, 348. (1976)
35. SC Kim et al., *Macromolecules,* 9,258m (1976)
36. Edward F Cassidy et al, *J.Polym.Sci.,* Polychem Ed, 22, 1839-1850 (1984)
37. H.Leidheiser.Jr., *Prog.Org.Coat.,* 7, 79, (1929)
38. W.Funke., *Prog.Org.Coat.,* 9,29, (1981)
39. W.Funke, *J.Coat.Technol.,* 62, 63 (1979)
40. W.Funke, *J.Coat.Technol.,* 55, 705, 31 (1983)
41. MW Kendig et.al., *Corr.Sci.,* 23,4,317-329 (1983)
42. AA Aksant et.al., *Corr.Sci.,* 22,7,611-619 (1982)
43. MW.Kendig et.al., *Corr.Sci.,* 23,9,1007-1005 (1983)
44. F Mansfeld, *Corrosion,* 36,5,301-307 (1981)
45. WJ.Loronz, et.al., *Corr.Sci.,* .21,9,647-672 (1981) ❑